Research

Preparation of a superior damping coating and study on vibration damping properties

Gen Jin[1,2] · Guo Chen[1,3] · Zihao Zhao[1] · Zhengda Zhao[2] · Lei Liu[2] · Jin Qian[1]

Received: 2 April 2023 / Accepted: 20 July 2023
Published online: 26 July 2023

Abstract
In this paper, a superior damping coating was prepared, which can be easily sprayed onto the samples, showing a promising application in the vibration reduction for aircraft. This paper aims to investigate the effect of filler content, size and coating thickness on the damping properties of aluminum flake samples. It is found that the vibration of the sample is significantly suppressed with the vibration reduction rate of the coating reaching 63.23%. Moreover, the damping ratio of the coating was calculated using the half-power bandwidth method, based on which the finite element simulation model was established. The simulation results are in perfect agreement with the test ones, and the maximum vibration amplitude error stayed within 9.06%. These results fully demonstrated the effectiveness and practicality of the damping coating.

Keywords Aircraft · Damping coating · Vibration reduction effect · Half-power bandwidth method · Finite element simulation

1 Introduction

The vibration problems of aircraft piping system have always been the focus of aircraft design [1]. Moreover, with the continuous development of modern aircraft pipeline systems toward large flow and high pressure, the problem of pipeline failure due to vibration is becoming increasingly prominent. According to the statistics made by the scholars from the United States, the failures of aircraft piping systems, such as fuel, air, and hydraulic systems account for 50–60% of the aircraft component failures. The statistical data of Russian aircraft also shows that the failures of aircraft pipeline systems account for more than half of the aircraft failures [2, 3]. The main forms of failures in aircraft piping systems include excessive vibration and vibration fatigue [4]. Excessive vibration is mainly caused by the resonance of the pipeline due to fluid or foundation excitation which directly causes large displacement of the joint surface between the pipeline fastener and the fixed part and results in surface friction or damage. The vibration fatigue of pipeline systems generally refers to the cumulative damage caused by the long-term operation of components, such as pipe bodies, pipe joints, and clamps in the working environment, and the crack growth and fracture after a certain number of cycles.

In general, there are two existing methods to control the vibration of the pipeline, that is, optimizing the shape of the pipeline and applying clamps to the pipeline [5]. The optimization of the shape of the conduit should be implemented mainly in the initial design stage, otherwise, it may consume a lot of resources to redesign and manufacture if the pipe is found to vibrate violently in actual

✉ Guo Chen, cgnuaacca@163.com | [1]College of Civil Aviation, Nanjing University of Aeronautics and Astronautics, Nanjing 210016, China. [2]Chengdu Aircraft Industrial (Group) Co., Ltd., Chengdu 610092, China. [3]College of General Aviation and Flight, Nanjing University of Aeronautics and Astronautics, Liyang 213300, China.

use. The application of clamp is the most widely used method, but in the meantime, it will inevitably increase the weight of the piping system. And more importantly, it is difficult to find a suitable position for the clamp in some narrow spaces. The recent development of damping coating provides an option for engineering vibration reduction [6–10]. Koshy and Alva et al. [11, 12] explored the effect of functional fillers on damping performance. Gao and Long [13] used a variety of inorganic materials as fillers, and found that when the material with layered structure is used, the damping performance and sound insulation performance of water-based damping coating can be significantly improved. Through the comparison of different fillers of the coating, including heavy calcium carbonate, mica powder, glass microbeads, silica, etc., Hu et al.[14] further found that the water-based damping coating with mica powder as the filler has the best damping performance. Zhang [15] used the free vibration attenuation method to evaluate the damping performance of the material. Gao et al. [16–18] provided theoretical support for the design and vibration control of complex pipeline systems, and pointed out that the passive vibration reduction technology of pipelines still needs to be further researched. Shlykov et al. [19] found the most appropriate percentage of organic fiber, and that there is a correlation between moduli and bending strength and the increase of fiber fraction. Yu et al. [20] discussed the damping efficiency of the coating system based on the Reuss model and Hashin-shtrickman equation. In addition, CHIBA et al. [21–24] proposed that sticking viscous damping material onto the outside the pipeline can effectively suppress vibration.

In this paper, a superior damping coating was proposed, of which the effectiveness and practicability were proved by simulation and experiment. The research results are of great application significance in reducing the vibration of aircraft pipelines. The novelty of this paper lies mainly in the fact that we obtained the optimal filler ratio and coating thickness by discussing the preparation of damping coatings. In addition, we calculated the damping ratio by using the half-power bandwidth method, and performed mutual verification based on the finite element simulation results, experimental results, etc., which are different from the previous efforts.

2 Experimental details

In this paper, 2A12 is selected as the substrate of coating with the dimension of 150 × 60 × 1 mm. The acrylic polyurethane emulsion, filler and functional additives, such as defoamer and leveling agent are mixed in turn by using the high-speed dispersing machine, as shown in Fig. 1. And the materials required for this experiment are listed in Table 1. At last, the damping coating is sprayed onto the substrate with a spray gun, and cured in an oven. As an important part of damping coating, the size and content of filler are important factors affecting the performance. In this paper, mica powder is selected as the main filler, with the sizes of 10 mesh, 40 mesh and 400 mesh, and the contents of 20%, 40%, and 60%, respectively. The coating thickness is set to less than 2 mm, because in practical engineering, the increase of coating thickness will lead to the increase of pipeline weight, resulting in reduction of economy.

In the vibration experiment, the clamping length of sample is controlled at 44 mm. Besides, the sine excitation method is used to sweep the frequency, and the

Table 1 Materials

Component	Name	Mass(g)
Latex	Acrylic polyurethane emulsion	500
Deionized water	Industrial distilled water	100
Filler	Mica powder	450
Defoamer	GM-25	20
Functional additive	RM2020	40
Dispersant	731A	30
Film forming aid	Alcohol ester twelve	40

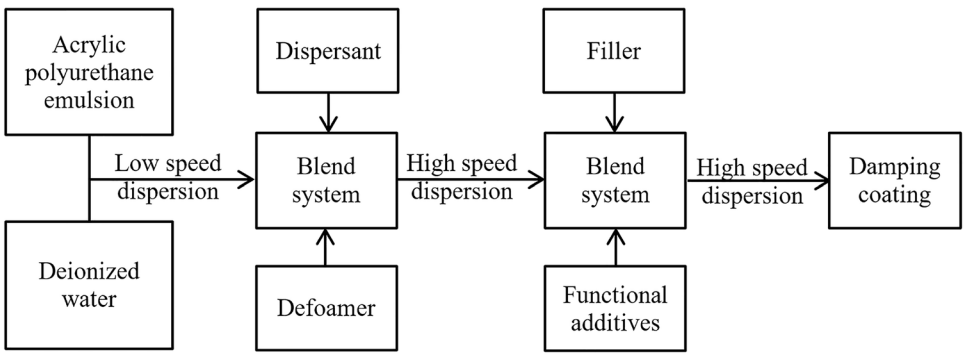

Fig. 1 The preparation process of damping coating

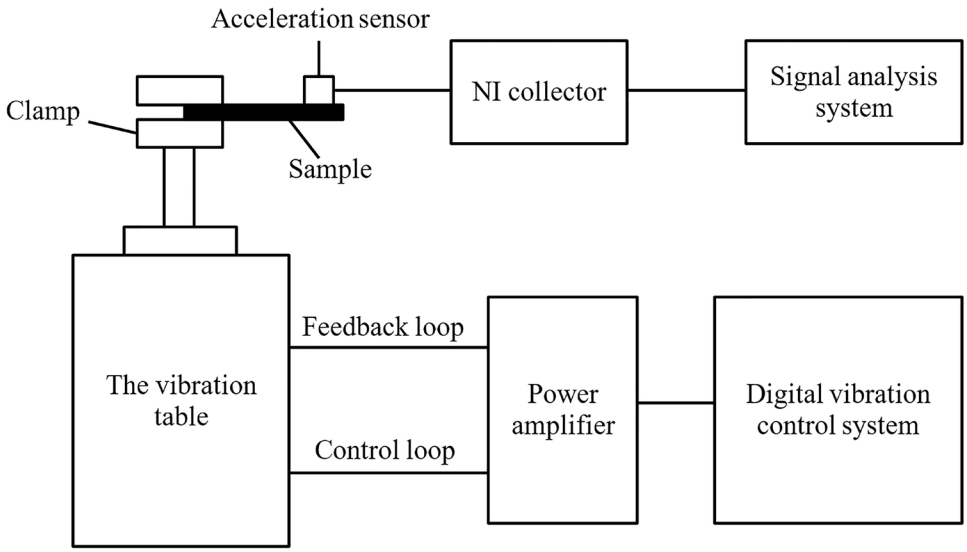

Fig. 2 The experimental principle

Table 2 Simulation parameters

Component	Density (kg/m^3)	Young's modulus	Poisson ratio
2A12	2800	6.6e10Pa	0.33
Sensor	7800	2.1e11Pa	0.30

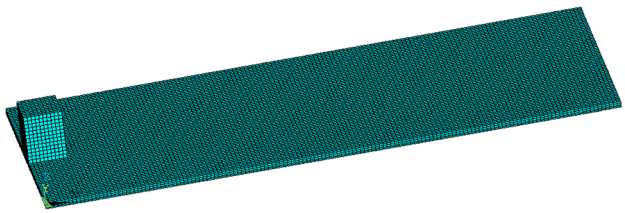

Fig. 3 The finite element simulation model

sweep frequency ranges from 0 to 80 Hz with the frequency interval of 1 Hz. Then, the basic excitation is applied by using the digital vibration control system, and the vibration acceleration of the sample is monitored by the acceleration sensor, so as to actively control the vibration. The above experimental principle is shown in Fig. 2.

Furthermore, in the simulation analysis, the finite element simulation model is established with the material parameters shown in Table 2. In addition, the material properties and acceleration sensor are both set in Hypermesh. After the model is completed, they are imported into Ansys.

The structure is unlikely to undergo plastic deformation under normal load, and it is even farther away from the plastic region in the test. Therefore, the linear elastic material constitutive model is used. During modeling, the substrate, damping coating, and sensor are considered as a whole, ignoring the connecting surfaces between them. In the meantime, SOLID185 unit is used to divide the above whole, and the established finite element simulation model is shown in Fig. 3. In addition, the viscoelastic properties of materials are represented by damping factor, which is related to the content and size of filler. The damping factor introduced in the model is calculated from the experimental data in Sect. 3.2 by the half-power bandwidth method.

3 Results and discussion

3.1 Vibration experiment analysis

Based on the above vibration signal analysis system, firstly, the vibration acceleration of the uncoated sample at the resonance is obtained as 38.22436 g. Secondly, the coated samples prepared using mica powder as filler, with the size of 10 mesh, 40 mesh and 400 mesh, and the content of 20%, 40% and 60%, respectively, are subjected to vibration test. Figure 4a–i illustrates the frequency spectrum of the vibration acceleration which, at the resonance of the sample with damping coating, is greatly reduced compared with that of the uncoated sample. The reason is that the addition of fillers increases the friction between polymer segments and fillers and that between fillers in the emulsion environment, thereby improving the damping performance of the sample, and achieving great reduction of the vibration acceleration.

In addition, it can be found that the vibration acceleration response of the coating with 20% filler is better than that of the coating with 60% filler when using different sizes mica powder as filler. This may be

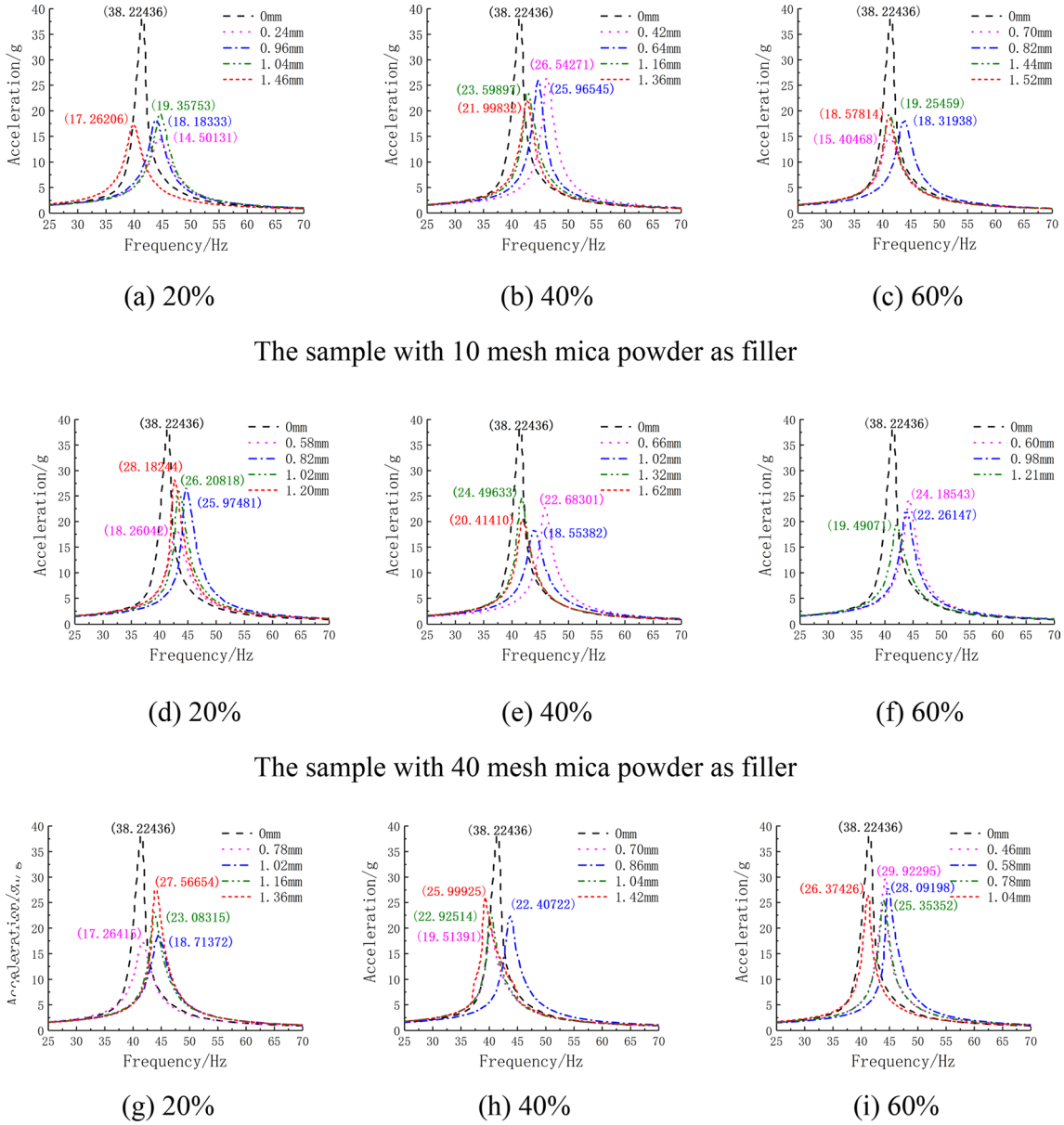

Fig. 4 Spectrum comparison of vibration acceleration

because when the filler content is low, the mica powder can be well dispersed in the emulsion environment, increasing the energy consumption between the polymer and the filler. When the filler content is high, on the one hand, mica powder is difficult to disperse uniformly in the emulsion environment, on the other hand, the energy consumption between polymer and polymer is reduced because of the decrease of polymer proportion, therefore, the damping properties of the coating decrease [15].

For the samples prepared with mica powder in the filler sizes of 10 mesh, 40 mesh and 400 mesh, respectively, the coating thickness and vibration acceleration are fitted, as shown in Fig. 5a–c. Seen from Fig. 5, when the size and content of mica powder are fixed, with the increase of coating thickness, the damping performance of the sample first increases and then decreases.

Furthermore, in Fig. 5a, when the coating thickness is low, the 60% content curve is between the 20 and 40% content curves, which differ from Fig. 5b, c. On the one

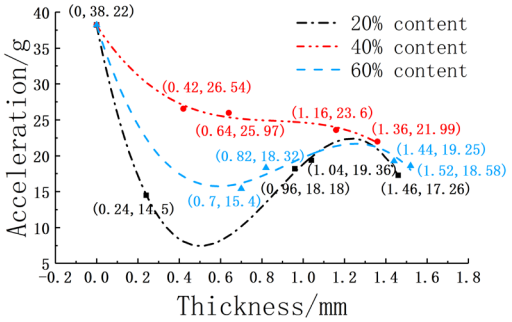

(a) The sample with 10 mesh mica powder as filler

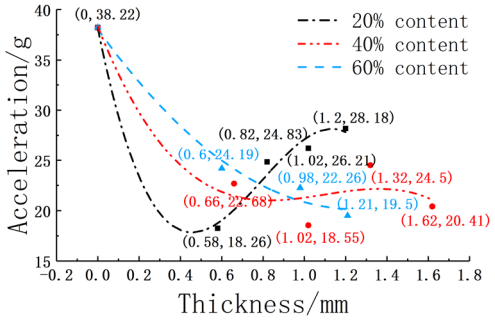

(b) The sample with 40 mesh mica powder as filler

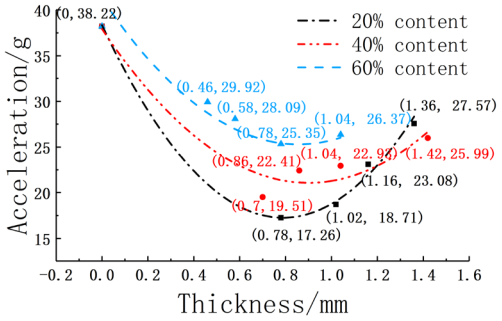

(c) The sample with 400 mesh mica powder as filler

Fig. 5 The influence of the coating thickness on the vibration acceleration

hand, this is the result of the experiment, on the other hand, this result proves that the factors affecting the damping performance of the coating include the content of polymer and filler, and the coating thickness, rather than a single factor.

In addition, Fig. 4 and Fig. 5 show that with the size of mica powder of 10 mesh, the content of 20%, and the coating thickness of 0.24 mm, the vibration reduction effect of the coating is the best, up to 63.23%. The reason is that the mica powder has a large particle size and a moderate content, which can better disperse in the emulsion, making the sliding of the lamella easier, converting more vibration energy into heat energy, and eventually achieving the superior vibration reduction effect [25].

3.2 Comparative analysis of experiment and simulation

The half-power bandwidth method is employed to analyze the spectrum obtained experimentally, and the damping ratio is calculated. Besides, the principle is as follows, the severe vibration of the system occurs not only at the resonance frequency, but also within a frequency band around it. In general, the amplitude amplification factor β_v is decreased to $1/\sqrt{2}$ of the peak value, and the interval corresponding to this frequency band is defined as the resonance region. To describe the intensity of resonance and the width of resonance region, the concept of system quality factor is introduced, as shown in Eq. (1):

$$Q^{def} = \frac{1}{2\zeta} = \beta_d\big|_{\lambda=1} = \beta_v\big|_{\lambda=1} = \beta_a\big|_{\lambda=1} \tag{1}$$

where Q^{def} represents the system quality factor, and ζ stands for the damping ratio.

Assuming that there are two endpoints, that is, A and B with the amplitude amplification factors of $Q/\sqrt{2}$ in the resonance region, their corresponding system power is exactly half of the corresponding power at the resonance frequency. Therefore, Point A and Point B are called half-power points. In addition, the square of the amplitude amplification factor at the half-power point can be expressed by using Eq. (2):

$$\beta_v^2 = \frac{\lambda_2}{(1-\lambda_2)+(2\zeta\lambda)^2} = \frac{Q^2}{2} = \frac{1}{8\zeta^2} \tag{2}$$

where β_v refers to the amplitude amplification factor.

Integrating both sides of Eq. (2) to obtain Eq. (3) and Eq. (4):

$$\lambda_A = \sqrt{1+\zeta^2} - \zeta \tag{3}$$

$$\lambda_B = \sqrt{1+\zeta^2} + \zeta \tag{4}$$

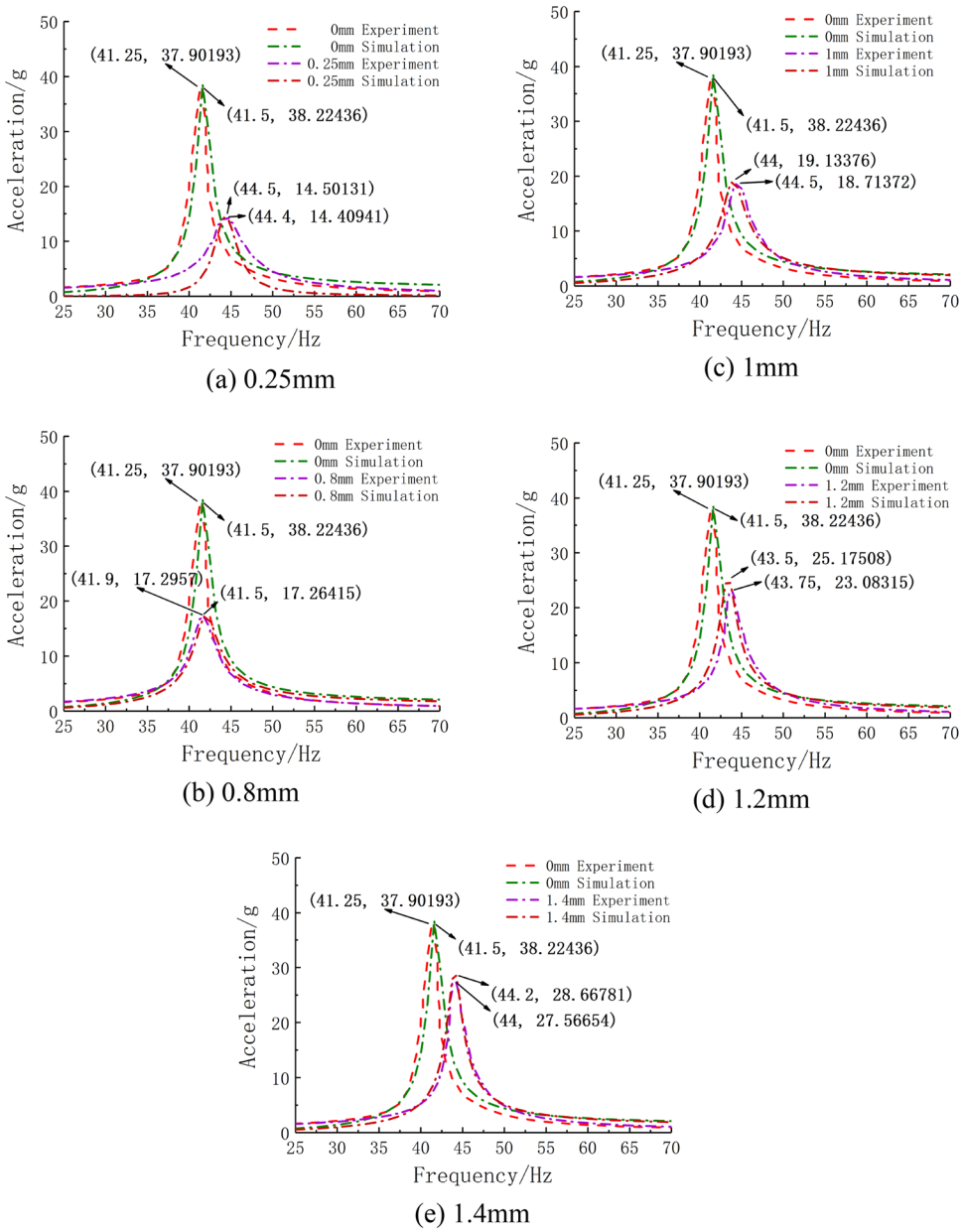

Fig. 6 Comparison between experimental data and simulation results

The bandwidth of the resonance region, also known as the half-power bandwidth, can be obtained by Eq. (5):

$$\Delta\lambda^{def} = \lambda_B - \lambda_A = 2\zeta = \frac{1}{Q} \tag{5}$$

It can be seen from the above results that in the case that the damping ratio is small, the quality factor is high, the resonance region is narrow, and the resonance peak is steep, vice versa. Then, we can get Eq. (6) from Eq. (5):

$$\zeta = \frac{\Delta\lambda}{2} \tag{6}$$

Draw a line in parallel with the frequency axis at 0.707 times of the formant. The straight line intersects the resonance curve at two points, and the abscissa values corresponding to these two points are recorded as f_1 and f_2, respectively.

Therefore, the damping ratio calculated according to the half-power bandwidth method is shown in Eqs (6, 7):

$$\zeta = \frac{f_2 - f_1}{2f} \times 100\% = \frac{\Delta f}{2f} \times 100\% \tag{7}$$

where f represents the actual resonance frequency, that is, the natural frequency.

Based on the half-power bandwidth method, at the particle size of mica powder of 400 mesh, the content is 20%, the coating thickness reaches 0.25 mm, 0.8 mm, 1 mm, 1.2 mm and 1.4 mm, and the corresponding damping ratios are 0.03933, 0.03313, 0.03089, 0.02286 and 0.01989, respectively. We substitute the obtained damping ratios into the finite element simulation model, and compare the results with the experimental data, as shown in Fig. 6.

As can be seen from Fig. 6, when the size and content of mica powder are fixed, the spectrum obtained by the simulation calculation is in perfect agreement with the experimental data, and the vibration amplitude errors are only 0.63%, 0.18%, 2.24%, 9.06%, and 3.99%, respectively. In a word, the above results prove the correctness of the experiment and the applicability of the half-power bandwidth method. In addition, these similar contents of the finite element methods and structural vibration are also mentioned in some recent additional pioneer works [26, 27].

4 Conclusions

In this paper, a superior damping coating was prepared, and its damping properties were discussed. During the research, firstly, the damping coating was prepared with acrylic polyurethane emulsion, filler and functional additives. Secondly, the effects of filler content, size and coating thickness on damping performance were analyzed, and the optimal formulation was obtained. Moreover, the damping ratio was calculated by using the half-power bandwidth method, and substituted into the finite element simulation model. In addition, the simulation results were compared with the experimental data. The specific conclusions of the entire paper were detailed as follows:

(1) The sample with damping coating has an obvious vibration damping effect compared with the uncoated sample. And when the size and content of mica powder are fixed, with the increase of the thickness of the damping coating, the damping performance of the sample will gradually reach the optimum.
(2) At the size of mica powder of 10 mesh, the content of 20%, and the coating thickness of 0.24 mm, the vibration reduction effect of the coating is the best, i.e., up to 63.23%.
(3) The error between the experimental data and the simulated data does not exceed 9.06%, proving the correctness of the experiment and the applicability of the half-power bandwidth method.
(4) The superior damping coating can effectively reduce the vibration of the pipeline system, which has significant theoretical significance and engineering practical value for effectively controlling the failure of the aircraft pipeline system and improving its safety and reliability.

Acknowledgements This work is supported by the National Natural Science Foundation of China (Grant No. 51675263), which is highly appreciated by the authors.

Author contributions Gen Jin and Zihao Zhao designed the research and wrote the original manuscript. Zhengda Zhao and Lei Liu analyzed data. Jin Qian reviewed and edited the manuscript. Guo Chen supervised the study. All authors read and approved the final manuscript.

Funding This study was supported by National Natural Science Foundation of China, No. 51675263.

Data availability The datasets generated during and/or analysed during the current study are available from the corresponding author on reasonable request.

Declarations

Competing interests The authors declare no competing interests.

References

1. Yu WG, Chen G, Liu BB et al (2018) Design of a particle damping absorber and experimental study on vibration damping of the pipe. Acta Aeronautica et Astronautica Sinica 39(12):401–413
2. Li ZZ, Gao PX, Zhao DZ et al (2017) Fault diagnosis and location of the aero-engine hydraulic pipeline based on Kalman filter. Adv Mech Eng 9(12):1–9
3. Zhang YL, Gao PX, Liu XF et al (2021) Fluid-induced vibration of a hydraulic pipeline with piezoelectric active constrained layer-damping materials. Coatings 11(7):757–768
4. Sang Y, Liu PK, Wang XD et al (2021) Fluid-structure interaction analysis of the return pipeline in the high-pressure and large-flow-rate hydraulic power system. Prog Comput Fluid Dyn 21(1):38–51

5. Li X, Wang SP (2013) Vibration control analysis for hydraulic pipelines in an aircraft based on optimized clamp layout. J Vib Shock 32(01):14–20
6. Li YC, Cheng B, Qiu M et al (2020) Tribological properties and corrosion resistance of MoS_2-based composite coatings with different graphene additions. China Mech Eng 31(20):2437–2444
7. Fan RP, Meng G, He CC et al (2008) Experimental study on viscoelastic damping materials for noise control in railway vehicles. J Vib Shock 27(06):123–127+192
8. Yang B, Yao Y, Huang HS et al (2015) Application of waterborne damping coatings in automobile industry. Paint Coat Ind 09:69–73
9. Inozume S, Aihara T (2021) Damping ratio maximization in thickness direction using viscoelastic and structural materials based on constrained layer damping. Eng Optim 54(3):539–551
10. Yating Z, Yong G (2021) Preparation and properties of EAA/C9 resin/natural rubber damping materials. China Plast Ind 49(5):116–119
11. Koshy AT, Kuriakose B, Thomas S et al (1994) Viscoelastic properties of silica-filled natural rubber and ethylene-vinyl acetate copolymer blend. Polym Plast Technol Eng 33(2):149–159
12. Alva A, Raja S (2011) Dynamic characteristics of epoxy hybrid nanocomposites. J Reinf Plast Compos 30(22):1857–1867
13. Gao YQ, Long XL (1973) Summary of trial production test of damping slurry. Railw Veh 12:9–34
14. Hu Z, Lei CL, Yang T (2012) Influence of fillers on aqueous damping coating. Paint Coat Ind 42(6):52–54
15. Zhang DJ (2015) Study on the effect of fillers on the damping properties of polymer materials. Harbin Engineering University, Harbin
16. Gao PX (2017) Vibration analyses of aero hydraulic pipeline system under multi-excitations and its constrained layer damping technology. Dalian University of Technology, Dalian
17. Wang B, Gao PX, Ma H et al (2021) A review on dynamic characteristics of aero-engine pipeline system. Acta Aeronautica et Astronautica Sinica 2021:1–25
18. Gao PX, Yu T, Zhang YL et al (2021) Vibration analysis and control technologies of hydraulic pipeline system in aircraft: a review. Chin J Aeronaut 34(4):83–114
19. Shlykov S, Rogulin R, Kondrashev S (2022) Determination of the dynamic performance of natural viscoelastic composites with different proportions of reinforcing fibers. Curved Layer Struct 9:116–123
20. Yu LM, Ma Y, Zhou CG et al (2005) Damping efficiency of the coating structure. Int J Solid Struct 42:3045–3058
21. Chiba T, Kobayashi H (1990) Response characteristics of piping system supported by viscoelastic and clasto-plastic dampers. J Press Vessel Technol 112(1):34–38
22. Fang J, Lyons GJ (1996) Structural damping of tensioned pipes with reference to cables. J Sound Vib 193(4):891–907
23. Johnson CD, Kicnholz DA (1982) Finite element prediction of damping in structures with constrained viscoelastic layers. AIAA J 20(9):1284–1290
24. Lepoittevin G, Kress G (2010) Optimization of segmented constrained layer damping with mathematical programming using strain energy analysis and modal data. Mater Des 31(1):14–24
25. Tan LH, Zhou ZC, He CC (2006) Study on dynamic mechanical properties of water-based damping coatings. Paint Coat Ind 36(11):5–7
26. Lenggana BW, Prabowo AR, Ubaidillah U et al (2021) Effects of mechanical vibration on designed steel-based plate geometries: behavioral estimation subjected to applied material classes using finite-element method. Curved Layer Struct 8:225–240
27. Tuswan T, Zubaydi A, Piscesa B et al (2022) A numerical evaluation on nonlinear dynamic response of sandwich plates with partially rectangular skin/core debonding. Curved Layer Struct 9:25–39